

# The combination of STDP and intrinsic plasticity yields complex dynamics in recurrent spiking networks

Andreea Lazar<sup>1,2</sup>, Gordon Pipa<sup>1</sup>, and Jochen Triesch<sup>1,3</sup>

1- Frankfurt Institute for Advanced Study  
Max-von-Laue-Str. 1, 60438 Frankfurt am Main - Germany

2- Center for Cognitive and Neural Studies (Coneural)  
Str. Saturn 24, 400504 Cluj-Napoca - Romania

3- University of California, San Diego - Cognitive Science  
9500 Gilman Dr. 0515, La Jolla, CA, 92093-0515 - USA

**Abstract.** We analyze the dynamics of deterministic recurrent spiking neural networks with spike-timing dependent plasticity (STDP) and intrinsic plasticity (IP) that changes the excitability of individual units. We find that STDP and IP can synergistically interact to produce complex network dynamics. These dynamics are quite different from the dynamics of networks that lack one or the other form of plasticity. Our results suggest that a synergistic combination of different forms of plasticity may contribute to cortical dynamics of high complexity, and they underscore the need to carefully study the interaction of different plasticity forms<sup>1</sup>.

## 1 Introduction

The Neocortex has been described as a device that mostly talks to itself [1]. Understanding the dynamics of recurrent cortical networks and how these dynamics give rise to cognitive functions is a central goal of neuroscience research. The dynamics of cortical circuits are shaped by a range of plasticity mechanisms operating at various time scales. Spike-timing dependent plasticity (STDP) is such a mechanism that has received much attention recently, e.g. [2]. Previous modeling studies have demonstrated that STDP can be used for the learning of spike sequences [3, 4, 5, 6]. In addition it has been shown that STDP closely corresponds to correlation analysis [7], which is an established system identification method.

In the brain, STDP is not the only form of plasticity and thus it may be important to study how various plasticity mechanisms interact. For example, it was recently shown that the function of Hebbian learning rules for continuous activation model neurons may be dramatically altered if Hebbian learning is accompanied by a so-called intrinsic plasticity (IP) mechanism that changes the intrinsic excitability of a neuron [8]. In particular it was shown that the two forms of plasticity may synergistically interact to allow the discovery of heavy-tailed directions in the input. Since IP appears to be a ubiquitous phenomenon

---

<sup>1</sup>This work was supported by the gemeinnützige Hertie-Stiftung.

in the brain, e.g. [9], we are interested in how it may interact with STDP to shape the dynamics of recurrent networks.

In the following we present a simple model of a recurrent spiking neural network that combines STDP and IP and we analyze the resulting dynamics of the network through computer simulations. We find that the two forms of plasticity interact to create network dynamics of high complexity.

## 2 The Model

We consider a recurrent network with  $N$  binary units. The firing activity of the network at the discrete time  $t \in \mathbb{N}$  is described by the activity vector  $\mathbf{x}(t) \in \{0, 1\}^N$ , where  $x_i = 1$  means that unit  $i$  is active (spiking) and  $x_i = 0$  means that the unit is inactive (not spiking). Units are connected through weighted synaptic connections  $\mathbf{W}$ , where  $W_{ij}$  is the connection from unit  $j$  to unit  $i$ . All connections are excitatory ( $W_{ij} \geq 0$ ) and self-connections are prohibited ( $W_{ii} = 0$ ). We define the *pre-activation*  $h_i$  of unit  $i$  at time  $t + 1$  as:

$$h_i(t + 1) = \left( \sum_{j=1}^N W_{ij}(t)x_j(t) \right) - T_i(t) - \max(x_i(t), x_i(t - 1)) , \quad (1)$$

where  $T_i(t)$  is the *threshold* of unit  $i$  at time  $t$ . The  $\max()$  term introduces a two-time step refractory period that effectively prevents unit  $i$  from becoming active for the two time steps immediately following a spike. The activity  $\mathbf{x}(t + 1)$  is defined as:

$$\mathbf{x}(t + 1) = \mathbf{kWTA}(\mathbf{h}(t + 1)) , \quad (2)$$

where  $\mathbf{h}(t + 1)$  is the vector of pre-activations, and  $\mathbf{kWTA}$  is the  $k$ -winner-take-all function that selects the  $k$  units with the highest activations and sets their activity to 1, while setting the activity of all other units to 0. This way there will be exactly  $k$  active units at each time step. Typically we choose  $k \ll N$ . This ensures *population sparseness*, i.e., only a small fraction of units are active at any time. We view the  $\mathbf{kWTA}$  mechanism as a crude but effective way of modeling the effect of a network of inhibitory interneurons.

We use a simple model of STDP that strengthens synaptic weight  $W_{ij}$  from unit  $j$  to  $i$  by a fixed amount  $\eta_{\text{STDP}}$  whenever unit  $i$  is active in the time step following activation of unit  $j$ . At the same time, the reciprocal connection  $W_{ji}$  is weakened by the same amount. Weights are constrained to the interval  $[0, 1]$  by clipping them if they would fall below 0 or grow beyond 1.

We incorporate a simple model of IP that individually adjusts the thresholds  $T_i$  of each unit. A unit that has just been active increases its threshold by a small amount while an inactive unit lowers its threshold:

$$T_i(t + 1) = T_i(t) + \eta_{\text{IP}}(x_i(t) - k/N) , \quad (3)$$

where  $\eta_{\text{IP}}$  is a small learning rate. This rule facilitates *life-time sparseness*, i.e., it drives each unit to be active on average  $k$  out of  $N$  times. This mechanism is complementary to the  $\mathbf{kWTA}$  mechanism that ensures *population sparseness*.

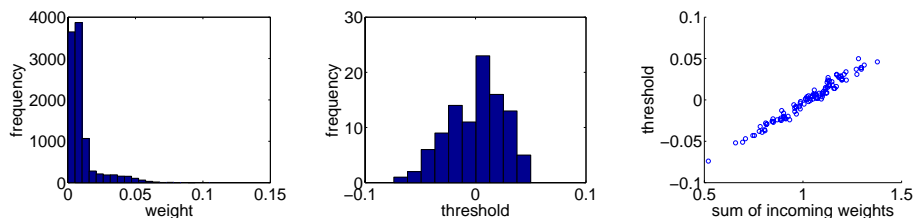


Fig. 1: Resulting structure of a network with  $N = 100$  and  $k = 10$  that was trained with STDP and IP. See text for details.

### 3 Experiments

#### 3.1 Emerging Network Structure

To characterize the emerging network structure we simulated the model for 10,000 time steps. The initial connectivity was such that 10% of all possible connections were initially present, and their strength were drawn from a uniform distribution over the interval  $[0, 1]$ . In this and all following experiments we used  $\eta_{\text{STDP}} = \eta_{\text{IP}} = 0.001$ .

Figure 1-**left** shows a typical histogram of the weight strength at the end of the simulation for a model with  $N = 100$  and  $k = 10$ . Note that the distribution is unimodal with most connections having small weights. The tail of the distribution extends to only slightly above 0.1, which was the maximum initial value for any weight. This emerging unimodal distribution of weight strength is quite different from the bi-modal distributions that are frequently observed in other models of recurrent networks with STDP. In Fig. 1-**center** we show the histogram of thresholds  $T_i$ . It assumes a unimodal shape centered at zero. The threshold value of individual units in the network becomes strongly correlated with the total synaptic drive they receive. This is illustrated in the scatter plot in Fig. 1-**right** that shows the threshold value of each unit as a function of the sum of weights projecting to the unit.

#### 3.2 Dynamics of Individual Units

To characterize the dynamics of the network we simulated it for an additional 10,000 time steps while gathering statistics of the firing patterns. Figure 2-**left** shows raster plots of the activity of all units during a 200 time step period. The average activity of the units over the entire simulation is narrowly distributed around  $N/k = 0.1$  due to the homeostatic nature of the IP mechanism, as shown in Fig. 2-**center**. The distribution of inter-spike intervals (ISIs) of the units (solid line in Fig. 2-**right**) is roughly exponential (compare dashed line) as would be expected from a Poisson process. There is a systematic shortage of very long ISIs and an abundance of relatively short ISIs, however. The power spectrum of unit activity is essentially flat (not shown), which is also consistent with a Poisson process. Note, however, that the dynamics of the network are

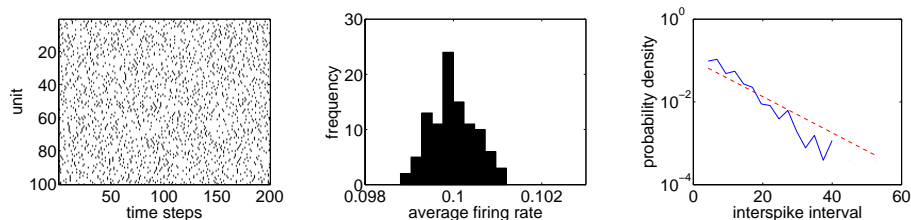


Fig. 2: Firing dynamics of individual units in a network with  $N = 100$  and  $k = 10$  that evolved under the influence of STDP and IP. See text for details.

completely deterministic.

### 3.3 Effect of STDP and IP on Network Dynamics

In order to study how STDP and IP contribute to the emerging network structure and dynamics we simulated networks with STDP and IP present or absent for varying  $N$  and  $k$ . Each simulation proceeded in two phases. During the *training phase* the network was simulated for 100,000 time steps with STDP and IP either switched on or off. In the subsequent *testing phase* we switched off all plasticity and analyzed the dynamics of the network<sup>2</sup>.

In the testing phase, the network state is fully described by the activity  $\mathbf{x}$  during the last two time steps. The number of possible states is given by  $(N!/(k!(N-k)!))^2$ . Since this number is finite, the network has to eventually enter a fixed point or a limit cycle. Fixed point solutions were never observed, a fact that is due to the units' refractory period that effectively prevents them from being active in two successive time steps. We estimated the number and length of limit cycles of the network as well as length of transient periods prior to reaching a limit cycle. Since the number of possible network states can be astronomically high, it is impractical to exhaustively search for all limit cycles by enumerating all states. Instead, we initialized each trained network in 100 random initial states and simulated it for 50,000 time steps while recording the history of states and monitoring for state repetitions that would indicate that the system had settled to a limit cycle of a particular period. Note that limit cycles whose period is longer than 50,000 time steps can not be detected by this method. We investigated how the limit cycle structure depends on  $N$  and  $k$  by training and analyzing 10 networks for each of a number of combinations of  $N$  and  $k$  values.

Figure 3 summarizes our results. We only present results for networks with  $N = 100$  and varying  $k$ . We also experimented with network sizes of  $N = 45$  and  $N = 20$  and the results are qualitatively similar, although they appear to get noisier for smaller  $N$ . In Fig. 3-left we plot the average length of the found limit cycles as a function of  $k$ . In the absence of STDP (dashed curves), the length of

<sup>2</sup>Switching off plasticity during testing allows us to analyze the dynamics for limit cycles because in this case the system only has a finite number of discrete states.

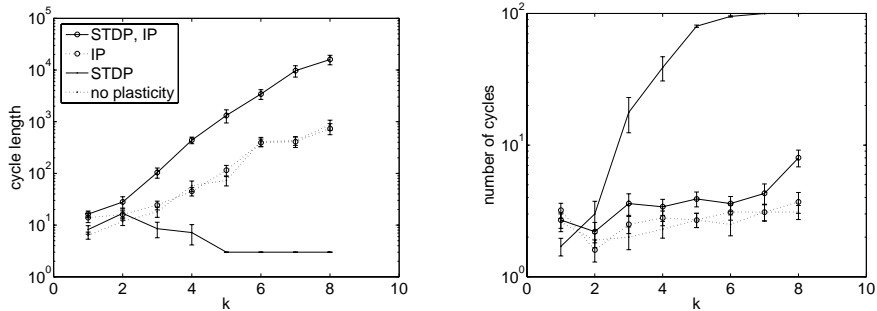


Fig. 3: Comparison of average length and average number of limit cycles in networks with  $N = 100$  and varying  $k$ , when trained with different combinations of plasticity mechanisms. Error bars indicate standard error of the mean. See text for details.

the found limit cycles tends to quickly grow as a function of  $k$ . The presence or absence of IP seems to play at most a minor role. When STDP is present (solid curves), however, the results are radically different depending on whether or not IP is accompanying the STDP. If IP is not present, the system exhibits limit cycles with very short periods. For  $k \geq 5$  the system virtually always runs into a limit cycle of period 3. In contrast, when STDP is accompanied by IP, the network develops very long limit cycles — even longer than those for networks without STDP whose synaptic connection matrix is completely random.

The number of distinct limit cycles we found by testing 100 random initial states of the networks is shown in Fig. 3-right. Again, if no STDP is present, it makes little difference whether IP is present or not. When STDP is present without IP, the number of limit cycles grows very quickly with  $k$  and saturates at 100, i.e., every starting state led to a distinct limit cycle. The length of the transient period, i.e., the time before these limit cycles are reached, tends to be at most a few steps (not shown), suggesting that these very short limit cycles fill a large fraction of the state space. When STDP and IP are combined, the number of distinct limit cycles that were found grows much more slowly with  $k$ , but still faster than for the cases without STDP. In this case the transient periods become very long and frequently the system does not re-enter any of its previous states within the testing time of 50,000 steps.

In sum, for networks trained with STDP only, the dynamics are characterized by a very large number of very short limit cycles that seem to fill a large fraction of the state space. In contrast, the networks trained with STDP and IP exhibit very long limit cycles — even longer than networks trained without STDP.

## 4 Discussion

We have studied the dynamics of a deterministic recurrent spiking network model and we investigated how these dynamics are shaped by the presence or absence of STDP and IP. Our major finding is that the effect of STDP on the network dynamics was radically different depending on whether it was accompanied by IP or not. While in the absence of IP, STDP leads to dynamics characterized by a large number of very short limit cycles, in the presence of IP it leads to a small number of very long limit cycles — even longer than those of randomly connected networks (with or without IP).

Our proposed network has a number of interesting features that may contribute to this behavior. It has two mechanisms to maintain homeostasis of its firing activity: the IP mechanism, which ensures lifetime sparseness of every unit, and the **kWTA** mechanism, which enforces population sparseness at every time. The absence of one or the other mechanism in previous models of recurrent networks with STDP may have prevented authors from observing similar kinds of dynamics and the emergence of a unimodal distribution of weight strength as we have. Note that our network is in fact completely deterministic in contrast to most previous recurrent network models with STDP. Nevertheless, it exhibits very complex dynamics with Poisson-like firing patterns in all units as also observed in certain randomly connected networks with balanced excitation and inhibition but without any plasticity [10]. More work is needed to address how different forms of plasticity may contribute to optimizing the computational properties of recurrent spiking networks.

## References

- [1] Valentino Braitenberg and Almut Schüz. *Anatomy of the Cortex*. Springer, 1991.
- [2] H. Markram, J. Lübke, M. Frotscher, and B. Sakmann. Regulation of synaptic efficacy by coincidence of postsynaptic APs and EPSPs. *Science*, 275(5297):213–215, 1997.
- [3] W.B. Levy. A sequence predicting CA3 is a flexible associator that learns and uses context to solve hippocampal-like tasks. *Hippocampus*, 6(6):579–590, 1996.
- [4] W. Gerstner and L.F. Abbott. Learning navigational maps through potentiation and modulation of hippocampal place cells. *J. of Computational Neuroscience*, 4(1):79–94, 1997.
- [5] D.A. August and W.B. Levy. Temporal sequence compression by an integrate-and-fire model of hippocampal area CA3. *J. of Computational Neuroscience*, 6(1):71–90, 1999.
- [6] R.P. Rao and T.J. Sejnowski. Spike-timing-dependent Hebbian plasticity as temporal difference learning. *Neural Computation*, 13(10):2221–2237, 2001.
- [7] R.E. Suri. A computational framework for cortical learning. *Biological Cybernetics*, 90:400–409, 2004.
- [8] Jochen Triesch. Synergies between intrinsic and synaptic plasticity in individual model neurons. In Lawrence K. Saul, Yair Weiss, and Léon Bottou, editors, *Advances in Neural Information Processing Systems 17*. MIT Press, Cambridge, MA, 2005.
- [9] W. Zhang and D. J. Linden. The other side of the engram: Experience-driven changes in neuronal intrinsic excitability. *Nature Reviews Neuroscience*, 4:885–900, 2003.
- [10] C. van Vreeswijk and H. Sompolinsky. Chaos in neuronal networks with balanced excitatory and inhibitory activity. *Science*, 274:1724–1726, 1996.